

Risk Maps for Cutter Tool Wear Assessment and Intervention Planning

J.G. Grasmick & M.A. Mooney
Colorado School of Mines, Golden, CO, USA

ABSTRACT: The risk assessment relating to geological and geotechnical conditions depends on the uncertainty in key parameters. However, understanding and communicating the spatial distribution of the uncertainty and corresponding risk is often a challenge. This paper presents a case study where three-dimensional risk maps were generated using site investigation data and spatial interpolation tools for the interpretation and communication of cutter tool wear risk. In addition, the maps are used to forecast the number of cutter tools requiring replacement during construction, which can serve as a decision aid for intervention planning. Construction data and observation logs are used to validate these maps and demonstrate how they can provide a more comprehensive assessment of tunneling risks.

1 INTRODUCTION

Soft ground tunneling projects often encounter rapid changing ground conditions that pose significant risks. However, deterministic geological profiles fall short of conveying the uncertainty in ground conditions along with the spatial extent of tunneling risks. The ability to model the spatial variability and uncertainty in geological/geotechnical conditions would improve the risk assessment, taking into consideration the spatial distribution of such risks and incorporating uncertainty in the geological profile. Geostatistical (or random field) methods can be employed to assess the spatial characteristics of the geological/geotechnical conditions and develop 3D models of variability and uncertainty (Chilès and Delfiner 2012; Pyrcz and Deutsch 2014).

In geotechnical engineering, spatial modeling of risks (i.e., risk maps) on both the project and city scale have increasingly gained attention in the literature. Huber et al. (2015) presented a spatial modeling approach for the risk-based characterization of an urban building site using geostatistical simulation methods. These maps aid in the communication of the allowable ultimate loads on the soil over the building site. Wang et al. (2017) used CPT data to map the spatial variability in liquefaction potential of soils on a city-wide scale for Christchurch, New Zealand. These risk maps have demonstrated to be effective in the communication of risks and serve as a decision tool for mitigation and planning.

This paper presents an example of employing geostatistical methods to develop 3D risk maps (or models). Site investigation data from the Northlink Tunnel project in Seattle, WA is used to map the risk for cutter tool wear. These risk maps allow for a more rigorous and comprehensive assessment of ground conditions. These maps also serve as a tool for improved communication between all parties on the risks faced in a particular project.

2 METHODOLOGY

Geostatistical methods are powerful tools used for spatial interpolation of geological features/geotechnical parameters. The spatial correlation/variability structure of these parameters

can be assessed and modeled using functions that quantify the correlation/variability as a function of distance and direction (e.g. auto-correlation functions, variograms, and Markov chains) (Chilès and Delfiner 2012; Carle and Fogg 1996). Both categorical (e.g., soil type) and continuous (e.g., geotechnical parameters) variables can be simulated using such models. Stochastic interpolation tools allow one to generate many statistically equally probable realization of the subsurface ground conditions. Post-processing these realizations derives average, most probable, uncertainty and other statistical measures spatially. The reader is referred to (Chilès and Delfiner 2012; Pyrcz and Deutsch 2014) for a more theoretical explanation of these methods.

In this paper, a transitional probability geostatistical method is used to simulate geology in terms of engineering soil units (ESU) in 3D. This method incorporates the conditional probabilities of a certain category (e.g., ESU) to occur adjacent to the others along particular directions. Proportions of each ESU, average lateral extend and thickness, connectivity and juxtaposition tendencies are also honored. In a sequential framework, conditional simulations are performed to generate many equally probable realizations of the ESU in the project extent. These simulations are conditioned to the site investigation data such that simulated values at locations where ESU samples were reported are equal to the observed ESU. The ESU simulation results (100 total) are post-processed to determine the most probable ESU profile, probabilities of particular ESUs to exist at any location, and uncertainty in the predicted (most probable) ESU based on the variability of simulated ESUs at each location.

Within the ESU model, geotechnical parameters are simulated using the sequential Gaussian simulation approach. In this approach, the spatial structure of relevant geotechnical data is inferred from the borehole data. The simulations are conditioned to the site investigation data as well as the ESU model. This allows one to take into account the different spatial characteristics and distributions of the geotechnical data within each ESU type. These simulation results are post-processed to determine the average and uncertainty in the geotechnical parameter of interest at any location. Figure 1 presents a flow chart of the general procedure for the geostatistical analysis described here.

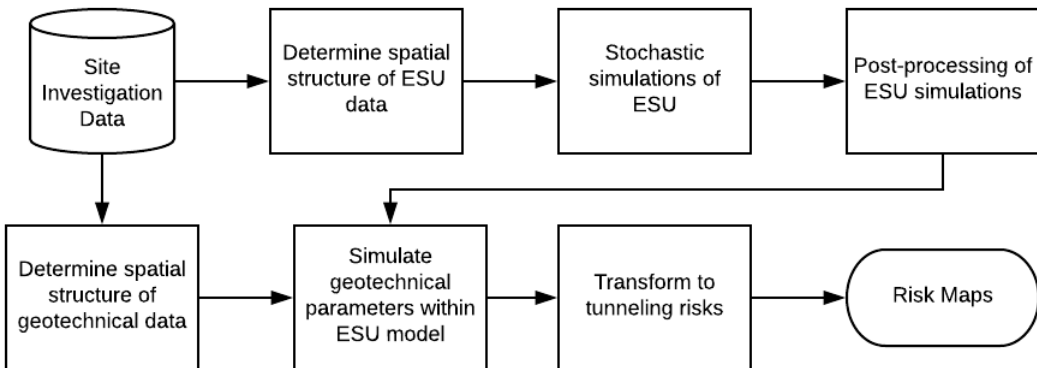


Figure 1. Flow chart of the procedure for developing risk maps.

3 PROJECT OVERVIEW

The Northgate Link tunnels project in Seattle, WA consisted of two (twin) tunnels, each approximately 5.6 km in length, excavated by 6.6 m diameter earth pressure balance tunnel boring machines (EPB TBM). The site investigation consisted of 158 boreholes with varying sampling methods for determining parameters including ESU classification, water content, Atterburg limits, grain size distribution, etc. The majority (58%) of the boreholes are within 50 m of another borehole. These boreholes are typically located at tunnel stations, where a higher density of boreholes is generally present. Along the tunnel drive (i.e., between stations), borehole spacing generally exceeds 50 m, and even 100 m in some cases. Figure 2 presents the spatial layout of the site investigation and the sampling frequency for ESU classification. The regional geology

consists of highly variable glacial and non-glacial sediments and according to the geotechnical baseline report, seven major ESUs are identified and summarized in Table 1 (Jacobs 2013).

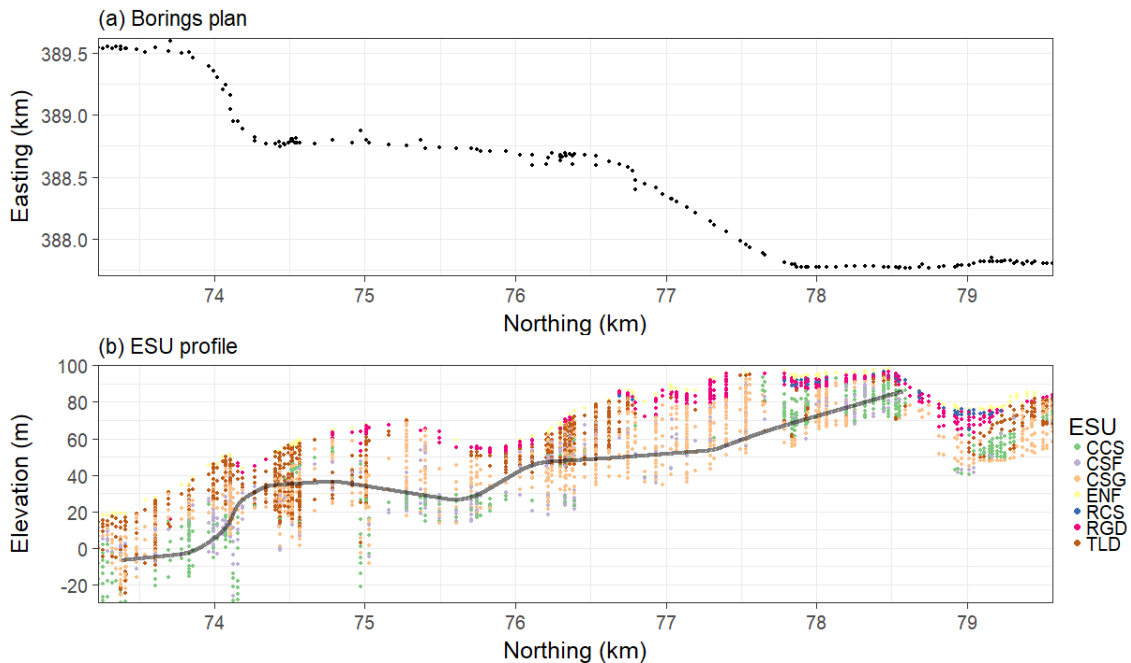


Figure 2. Overview of tunnel site and site investigation data. a) Plan view with borehole locations; b) Profile view of reported ESU samples.

Table 1. Description of Engineering Soil Units encountered in project area.

Engineering Soil Unit	USCS	Description
Cohesive Clay and Silt (CCS)	CH, CL, MH, ML, OH, OL, PT, SC, SM	Hard, interbedded silt and clay. Includes multiple layers and lenses of cohesionless silt, sand, and gravel, with varying lateral extent and thickness.
Cohesionless Silt and Fine Sand (CSF)	ML, SM, SP	Fine-grained granular soil consisting of very dense silt, fine sandy silt, and silty fine sand.
Cohesionless Sand and Gravel (CSG)	GM, GP, SM, SP, SW	Dense to very dense silty sand to sandy gravel. May contain lenses of clay and clayey silt.
Engineered and Non-Engineered Fill (ENF)	CL, GM, GP, ML, OH, OL, SC, SM, SP, SW	Very loose to very dense sand with varying amounts of silt and gravel. Also includes wood, concrete, metal, brick, and other debris.
Recent Clay and Silt (RCS)	CH, CL, ML, OL, PT, SC, SM	Soft to stiff silty clay and clayey silt with variable amounts of sand and gravel in localized zones.
Recent Granular Deposits (RGD)	GC, GM, GP, ML, SM, SP	Loose to dense or locally very dense silty sand, medium stiff to hard sandy silt, and silt. Contains localized lenses of sandy gravel and gravelly sand with varying lateral extent and thickness.
Till and Till-Like Deposits (TLD)	CL, GC, GM, GP, GW, ML, SC, SM, SP, SW	Has a high spatial variability and will grade over short distances from an unsorted mixture of gravel, sand, silt, and clay, to an unsorted mixture of silt, sand, and gravel to clean or relatively clean sand and gravel.

4 CUTTER TOOL WEAR RISK MAP

To illustrate risk map development, an example for cutter tool wear is presented. We rely upon tool wear prediction models from Koppl et.al, (2015) in this analysis. However, the approach can be applied using a variety of different tool wear prediction models. According to Koppl, et.al, the rate of cutter tool wear in soft ground tunneling is a function of the soil abrasivity index (*SAI*):

$$SAI = \frac{EQC}{100} * \tau_c * D_{60} \quad (1)$$

where *EQC* is the equivalent quartz content (%), τ_c is the Mohr-Coulomb shear stress (kN/m²) and D_{60} is the grain size where 60% of all grains are finer (mm). From the site investigation data relating to relevant geotechnical parameters EQC, τ_c and D_{60} , the distributions of SAI for each ESU can be determined. Boxplots representing the distribution of SAI for each ESU is presented in Figure 3. As expected, CSG and TLD exhibit higher SAI compared to other ESUs due to the presence of gravel and cobbles.

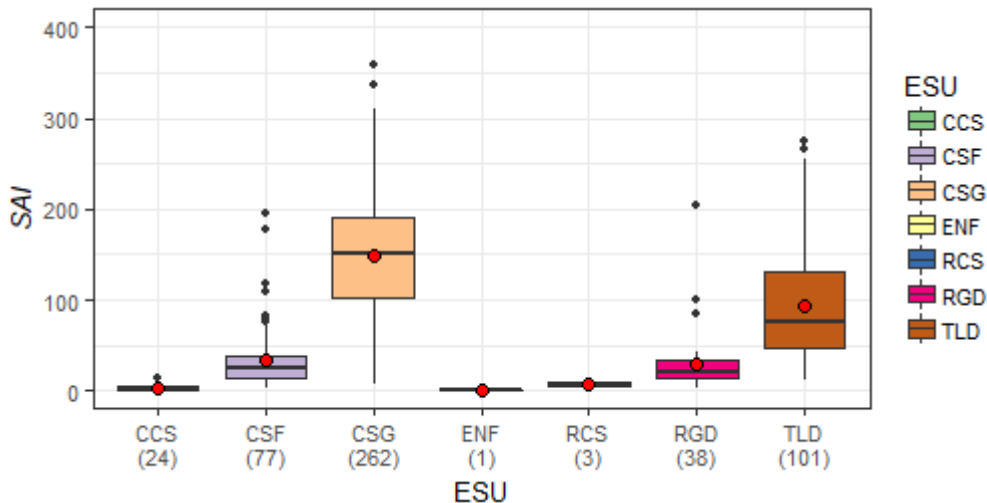


Figure 3. Boxplot of *SAI* parameter for each ESU. The number in parentheses corresponds to the number of samples available from the site investigation.

In the geostatistical simulation, 10,000 individual, statistically possible realizations of the ground conditions were generated. The results of the geostatistical simulation is summarized in Figure 4. Here, the average predicted *SAI* and corresponding uncertainty (in terms of standard deviation σ_{SAI}) along the tunnel axis is presented. Examination of the profiles reveals that *SAI* can vary significantly over the alignment, including drastic changes in *SAI* over short (< 100 m) distances. In addition, the uncertainty in *SAI* is quite variable along the alignment. Regions of high uncertainty imply that actual *SAI* is not well understood locally, and is a result of a combination of limited sampling and local variability in the geotechnical data.

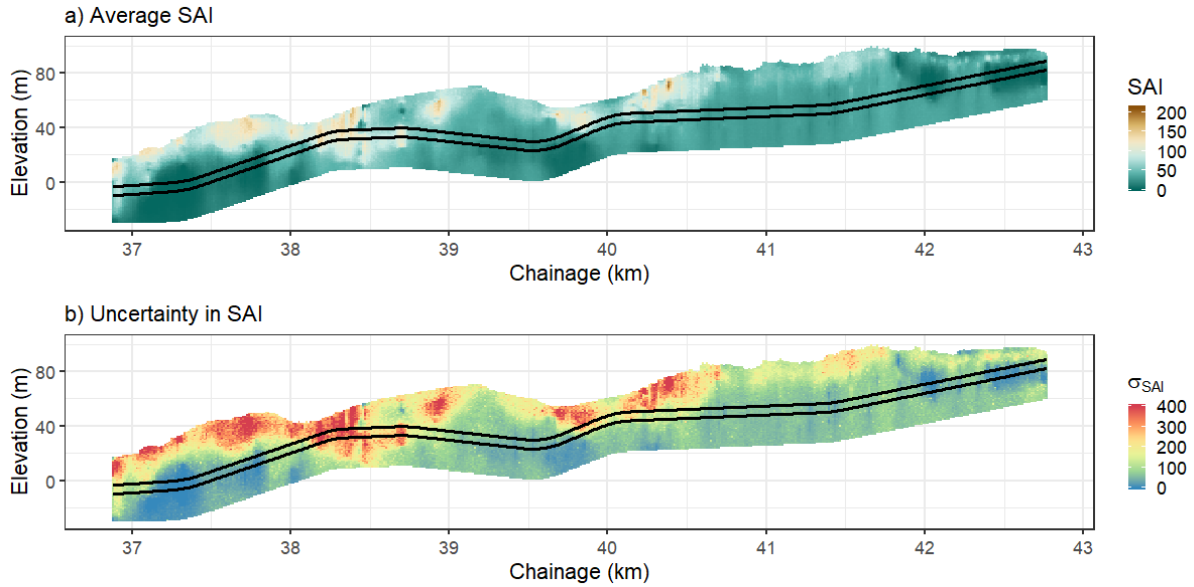


Figure 4. Results of the geostatistical simulation for *SAI*. a) Average *SAI*; b) Uncertainty in *SAI*.

The range and average predicted *SAI* within the tunneling horizon (excavated ground) from the risk map is presented in Figure 5. The deterministic estimate of *SAI* is also plotted for comparison. It can be observed that the change in *SAI* can vary significantly over ~250 m of excavation. In general, the geostatistical model predicts lower *SAI* compared to the deterministic estimate, with the exception of chainage 38.2–38.7 km, 39.5 km and, to some degree, 39.9–40.2 km. At chainage 40.5–42 km, the deterministic approach predicts significantly higher *SAI* than the geostatistical model. This is a section of the tunnel alignment where predominately CSG soils are encountered. The deterministic approach utilized the deterministic geological profile in the GBR and takes the average *SAI* of all samples for the respective ESU, rather than considering the regional distribution at any section of the tunnel alignment. The geostatistical model reveals that the average *SAI* in the 40.5–42 km region within the tunnel horizon is actually significantly lower than the average of all *SAI* samples for CSG.

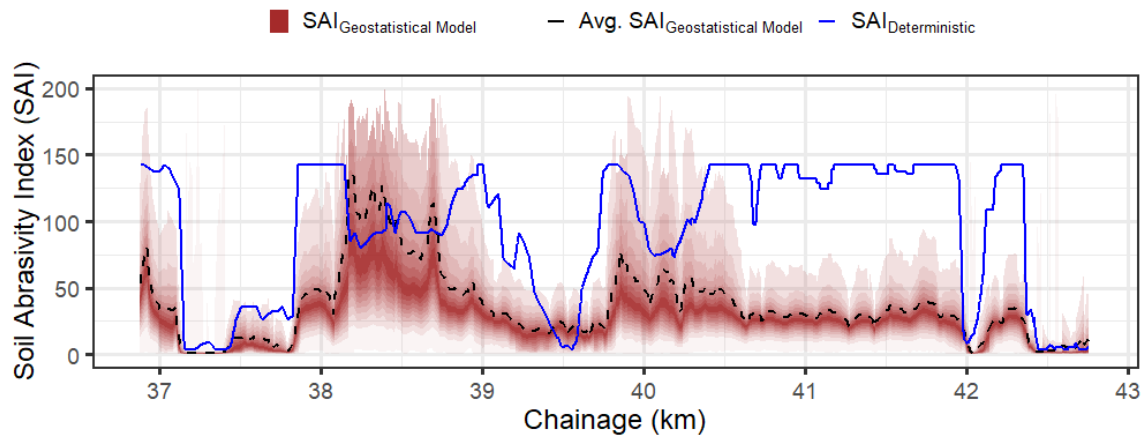


Figure 5. Range and average predicted *SAI* within the tunnel horizon (crown/invert). The estimated *SAI* using a deterministic approach based on the geotechnical baseline report (GBR) geological model is presented for comparison.

To estimate the number of cutter tool replacements during TBM excavation, we adopt the equations proposed in Koppl et.al, (2015). To estimate the expected cutting distance s_c for each of the tools based on the geostatistical model, the predicted *SAI* for each realization of the simulation is used. For each ring, the average s_c within the tunnel horizon for each realization closest to the respective ring is taken and divided by the actual cutting distance s_{cd} for each of the cut-

ting tools (using the average penetration rate p_e for the respective ring) to get the partial utilization factor e_{cd} . Figure 6 presents the average and 95% probability interval (PI) of the cumulative number of tool replacements N vs. ring number according to the geostatistical model. The deterministic estimation according to the GBR geological model is also plotted for comparison. For both cutting tool types, the geostatistical model on average predicts fewer tool replacements than the deterministic model. Furthermore, comparison with recorded tool replacements from the project validates the geostatistical model estimates and demonstrates the approach presented in this paper performs better than the deterministic estimate.

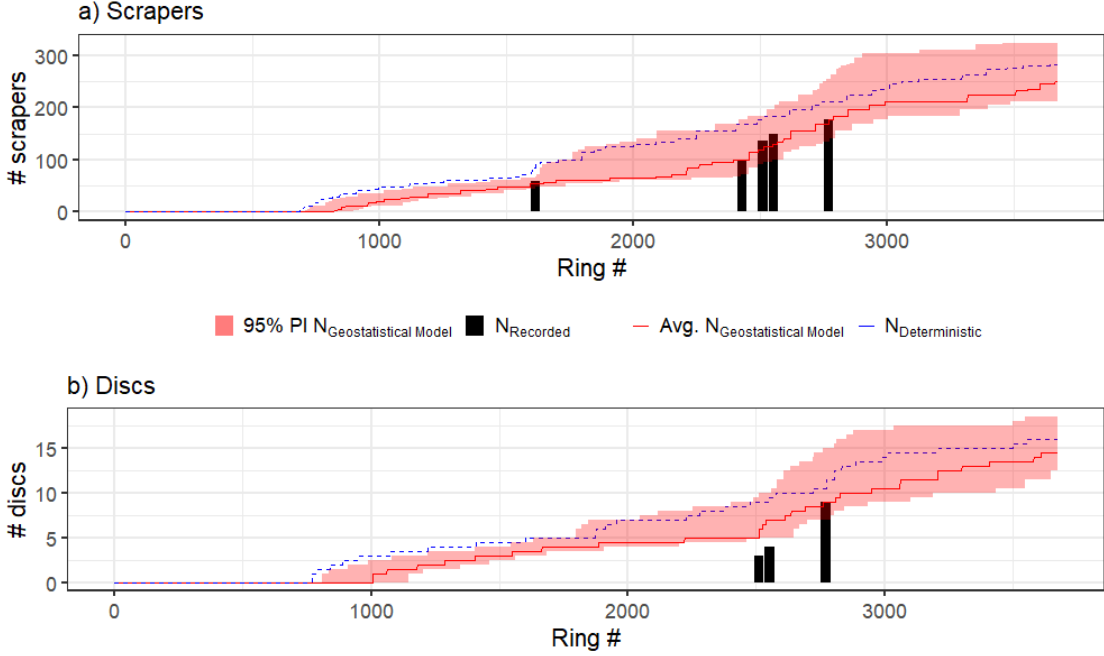


Figure 6. Estimated cumulative tool replacement for (a) scrapers and (b) discs compared with the deterministic estimate and the recorded tool changes during the project.

5 CONCLUSIONS

Geostatistical methods have been widely adopted in industries such as mining, petroleum/gas, hydrology and environmental engineering. However, few efforts have been made to extend these tools to heavy civil applications such as tunneling (particularly in soft ground). The example presented in this paper demonstrates the added value of performing geostatistical analysis on site investigation data for a more rigorous/comprehensive risk assessment. The key advantages of applying geostatistical methods are 1) to determine spatial characteristics/trends in the data and 2) quantify uncertainty in ground conditions.

Through validation with field records, the results of the risk mapping presented here demonstrate to provide more accurate estimates of the ground conditions. As a result, estimates of cutter tool replacements are significantly improved. Furthermore, quantifying spatial uncertainty in the ground conditions provides a direct means for quantifying the uncertainty in the required mitigation to account for risks. This information can serve as an aid for improved intervention planning.

The outcomes of the geostatistical analysis and the development of the risk maps can serve as communication tools to key stakeholders of a project. This approach can be applied to a range of other tunneling risks including clogging, ground deformation, and mixed face conditions, among others. 3D models such as those presented in Figures 7 and 8 can aid in procurement, establishing baselines, design and risk mitigation planning. Site investigation data is often underutilized. Applying geostatistical methods enables us to extract the most information out of the

data, and better convey areas where further site investigations and/or mitigation measures may be warranted.

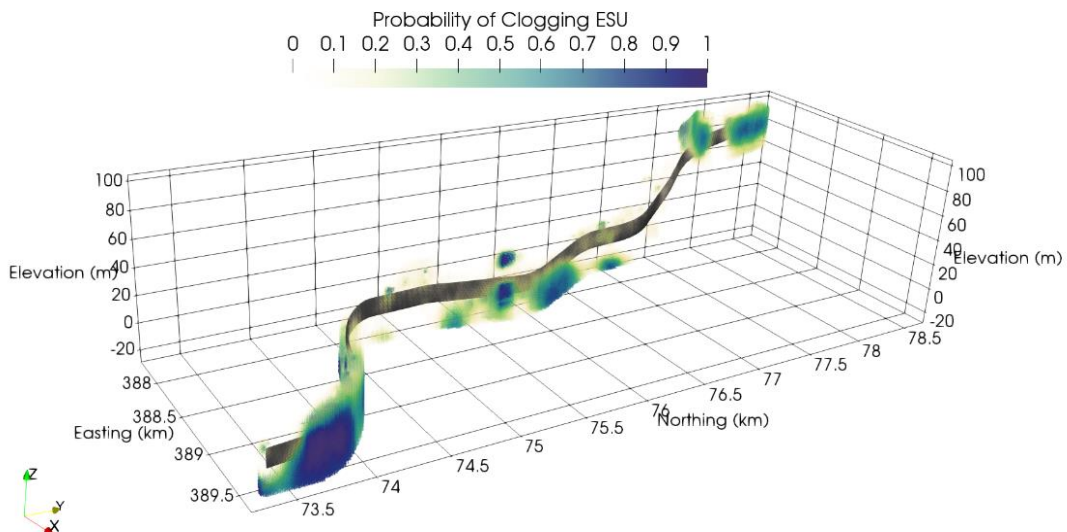


Figure 7. 3D risk map of the probability for clogging ESUs.

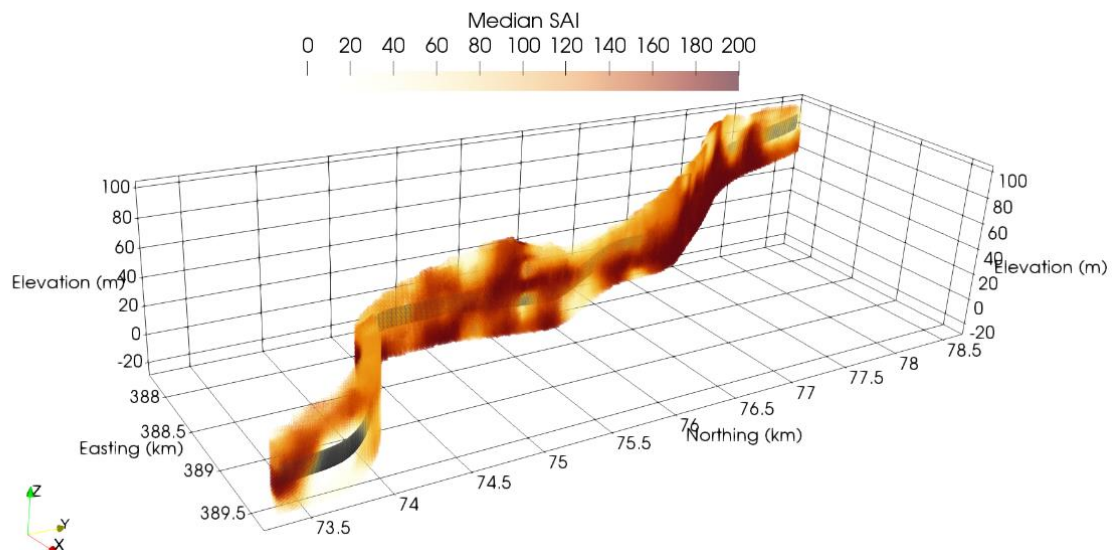


Figure 8. 3D risk map of soil abrasivity index.

REFERENCES

- Carle, S. F., & Fogg, G. E. (1996). Transition probability-based indicator geostatistics. *Mathematical Geology*, 28(4), 453-476.
- Chiles, Jean-Paul, and Pierre Delfiner. *Geostatistics: Modeling Spatial Uncertainty*. Wiley, 2012.
- Huber, M., Marconi, F., & Moscatelli, M. (2015). Risk-based characterisation of an urban building site. *Georisk: Assessment and Management of Risk for Engineered Systems and Geohazards*, 9(1), 49-56.
- Jacobs, A. (2013). "Northgate Link Extension Light Rail Project Contract N125: TBM Tunnels (UW to Maple Leaf Portal) Geotechnical Baseline Report."

- Köppl, F., Thuro, K., & Thewes, M. (2015). Suggestion of an empirical prognosis model for cutting tool wear of Hydroshield TBM. *Tunnelling and Underground Space Technology*, 49, 287-294.
- Maidl, B., Herrenknecht, M., Maidl, U., & Wehrmeyer, G. (2013). *Mechanised shield tunnelling*. John Wiley & Sons.
- Pyrcz, M. J., & Deutsch, C. V. (2014). *Geostatistical reservoir modeling*. Oxford university press.
- Wang, C., Chen, Q., Shen, M., & Juang, C. H. (2017). On the spatial variability of CPT-based geotechnical parameters for regional liquefaction evaluation. *Soil Dynamics and Earthquake Engineering*, 95, 153-166.